AUTOMATIC TOOTH SEGMENTATION USING ACTIVE CONTOUR WITHOUT EDGES

Samir Shah, Ayman Abaza, Arun Ross and Hany Ammar

West Virginia University, Morgantown, WV 26506 USA
{sshah, ayabaza, ross, ammar}@csee.wvu.edu

ABSTRACT

Automating the postmortem identification of deceased individuals based on dental characteristics is receiving increased attention especially with the large number of victims encountered in mass disasters. An automated dental identification system compares the teeth present in multiple digitized dental records in order to access their similarity. The primary step in such a system is the estimation of the contour of each tooth in order to permit efficient feature extraction. Extracting the contour of the teeth is a very challenging task and has received inadequate attention in the literature. In this paper, the task of teeth contour extraction is accomplished using active contour without edges. This technique is based on the intensity of the overall region of the tooth image and, therefore, does not necessitate the presence of a sharp boundary between teeth. Further, this technique can extract the region contour in the presence of additive noise and in the absence of well-defined image gradients. Experimental results indicate the benefits of the proposed approach.

1. INTRODUCTION

Forensic Odontology is a branch of forensic science that applies dental knowledge to civil and criminal investigations. Dental features are primary candidates for Postmortem (PM) human identification, since they resist the early decay of body tissues and withstand severe environmental conditions [1]. In 1997, the Criminal Justice Information Services (CJIS) division of the FBI created a Dental Task Force (DTF) to foster the creation of an Automated Dental Identification System (ADIS) [2]. The schematic diagram of such a system is illustrated in Figure 1. ADIS is expected to provide automated search and matching capabilities for digitized radiographs and photographic dental images so as to generate a short match list that would assist dental forensic experts in identifying (deceased) individuals. Recent work in ADIS reveals three challenging segmentation problems. First, the digitized dental X-ray record of a person often consists of multiple films, as shown in Figure 2(a). Thus, the *global* segmentation problem consists of cropping a composite digitized dental record into its constituent films [3, 4]. Second, each cropped film will contain multiple teeth, as shown in Figure 2 (b). The *local* segmentation problem involves isolating each tooth segment (as a rectangular entity) in order to facilitate the subsequent extraction of features like contours of the crown and root [1] for tooth classification and identification. Third, the contour of each tooth has to be estimated from individual isolated segments. Extracting the contour of an individual tooth is a very important step in automated dental classification and identification. In [5], Jain and Chen, propose a semi-automatic contour extraction method. The crown center is first marked within the tooth segment and an edge detection procedure is used to extract the contour of teeth. In [6], Chen and Jain extract the teeth contour using active contour models. They introduced a new dynamic energy term that permitted the directional snake [7] to discriminate the boundary between adjacent teeth. Zhou and Abdel-Mottaleb [8] also used active contour models (based on snakes) for extracting the contour of the teeth. Active contour models based on edges are driven by the gradient of the image intensities. In many dental images, the gradient between the teeth and the background is not prominent and, hence, such techniques will not be able to accurately extract the tooth contour. Also, snake-based schemes rely on a parametric representation of the contour. Parametric representations typically fail to evolve in noisy conditions [9]. Further, parametric contours may not be able to split and merge upon encountering local minima in the region of interest ([10], [11], [12], [13]). To address this limitation, Chan and Vese [14] proposed a novel technique using active contour without edges based on the Mumford-Shah functional for image segmentation [15]. In this paper the active contour without edges technique is utilized to trace the contour of the teeth. This technique is observed to be robust to discrepancies in the gradient of the images. Moreover, since it is based on the characteristic of the overall region of the tooth image, it is possible to extract a very smooth and accurate tooth contour using this technique. The initial contour can reside in any part of the image and does not have to be in the vicinity of the boundary of the tooth as is necessary in the case of snakes. Experimental results on dental images confirm the efficacy of the technique.

[1] The crown is the part of the tooth that lies above the gum line while the root resides below the gum line.

1-4244-0487-8/06/$20.00 ©2006 IEEE

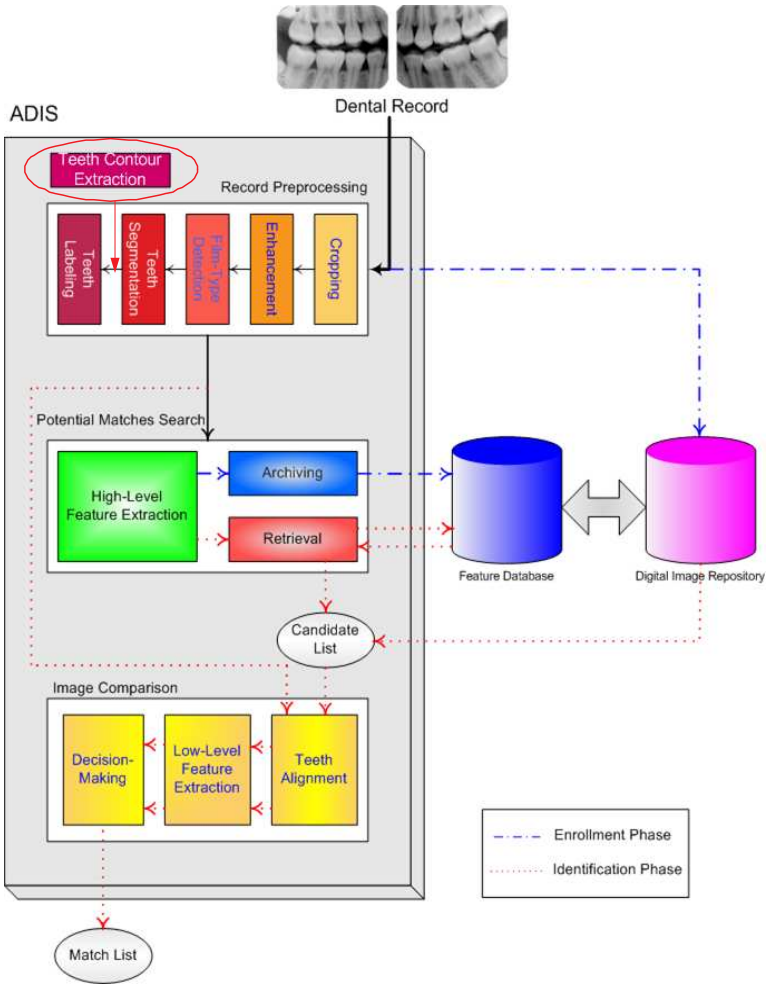

Fig. 1. Block diagram of ADIS.

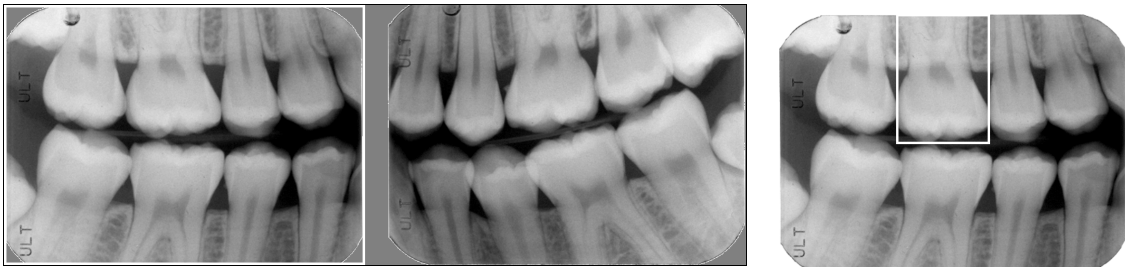

(a) (b)

Fig. 2. ADIS segmentation:
(a) Global segmentation (cropping on the film corners); (b) Local segmentation (teeth isolation).

1-4244-0487-8/06/$20.00 ©2006 IEEE

2. TEETH CONTOUR EXTRACTION USING ACTIVE CONTOURS WITHOUT EDGES

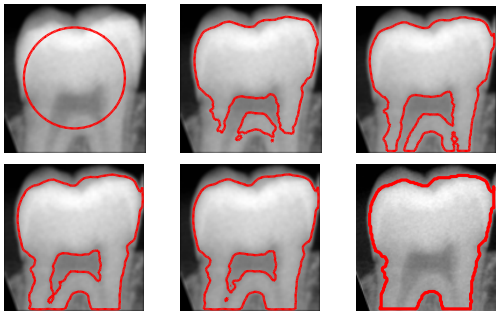

Fig. 3. Evolution of the active contour without edges.

The dental X-ray film is assumed to be a gray-scale image denoted by $X(i,j) \in [0,255]$ where $(i,j) \in \Omega = [1,H] \times [1,W]$ (H, W are the height and width of the film). To detect the contour of a tooth, a novel method based on active contours without edges [14] has been used. This is a region based segmentation technique where the evolution of the contour is guided by a model fit error term. The image is assumed to be made of two regions, viz., the foreground and background of approximately piecewise constant distinct intensities say I_0^0 and I_0^1, respectively. Let C_0 be the contour separating the two regions. Let the energy of the fitting be defined as

$$E(C) = \int_{inside(C)} |I_0(x,y) - c_1|^2 dxdy + \int_{outside(C)} |I_0(x,y) - c_2|^2 dxdy \quad (1)$$

where C is any contour in the image, and c_1 and c_2 are the mean intensities of the image, I_0, inside and outside of the contour C, respectively. The above equation will be minimized only when the contour $C = C_0$, i.e., when the contour C is segmenting the boundary of the object. It will be non-zero when the contour is either inside or outside the object. Let ψ be defined as a signed distance function from the curve C. Thus,

$$\psi(x,y) = \begin{cases} 0 & \text{if (x,y) is on the curve;} \\ < 0 & \text{if (x,y) is inside the curve;} \\ > 0 & \text{if (x,y) is outside the curve.} \end{cases} \quad (2)$$

ψ is the implicit representation of the curve C and is called as the embedding function as it embeds the evolution of C. The embedding function evolves from inside the tooth image under the influence of the above mentioned model fit error term. It terminates on the boundary of the tooth. The contour is initialized as a circle at the center of the image. The evolution equation is then given by [14]:

$$\frac{\partial \psi}{\partial t} = [\mu div(\frac{\triangle \psi}{|\triangle \psi|}) - (\lambda_1 (I_0 - c_1)^2 + \lambda_2 (I_0 - c_2)^2)],$$

where λ_1, λ_2 and μ are constants[2]. The first term (curvature of the curve), $div(\frac{\triangle \psi}{|\triangle \psi|})$, is calculated as:

$$div(\frac{\triangle \psi}{|\triangle \psi|}) = -\frac{\psi_{xx}\psi_y^2 - 2\psi_x\psi_y\psi_{xy} + \psi_{yy}\psi_x^2}{(\psi_x^2 + \psi_y^2)^{\frac{3}{2}}},$$

where ψ_x is the gradient of the image in the x direction; ψ_y is the gradient in the y direction; ψ_{xx} is the 2^{nd} order derivative in the x direction; ψ_{yy} is the 2^{nd} order derivative in the y direction; and ψ_{xy} is the 2^{nd} order derivative first in the x direction and then in the y direction. The curvature term provides the smoothing constraints on the evolution of the contour by minimizing the total curvature of the contour. The second term, the model fit error term, drives the evolution of the contour. The model fit error is minimized when the contour divides the image in such a way that the mean intensities c_1 and c_2 have the maximum difference. Thus, sharp edges are not necessary for the successful operation of the algorithm.

In some dental images a part of the neighboring tooth may also be erroneously included in the segmented result (note that local segmentation precedes the contour extraction process). To eliminate this, a post processing step was used after contour extraction. The contour on the left and right side of the tooth is always convex in shape. Hence, whenever the contour assumes a concave shape due to the erroneous inclusion of a neighboring tooth image, that portion of the contour is deleted.

3. EXPERIMENTAL RESULTS

The aforementioned procedure was used to extract the teeth contour of images from CJIS Division's Digitized Radiographic Images database [16]. This database has two types of dental radiographs. The radiographs obtained when the person is alive are labeled as Ante-mortem (AM) radiographs and those obtained after the death of the person are labeled as Post-mortem (PM) radiographs. From this database a total of 10 AM and 10 PM records were randomly selected. Each record contains approximately 3 films. There is a total of 340 teeth represented in these films. The tooth contour extraction algorithm was executed on these images and the results were manually categorized into the following four types: (a) Perfectly segmented tooth (whole tooth) (P), (b) Perfectly segmented crown (PC), (c) Contour that can be corrected at a later stage (C), (d) Error in contour extraction (E). Figure 4 shows examples for each of the above mentioned categories.

[2]In our implementation, $\lambda_1 = \lambda_2 = 1$ and $\mu = 2$.

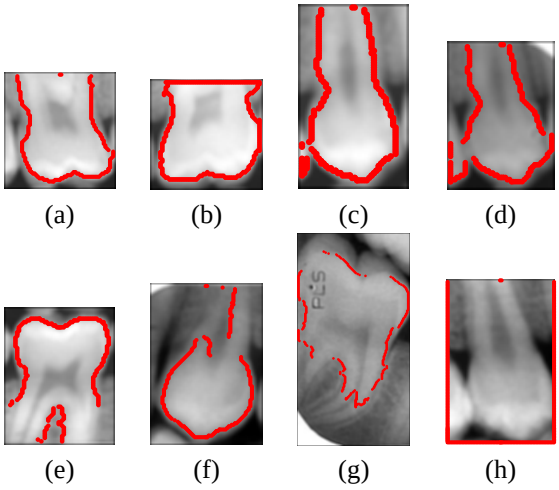

Fig. 4. Contour extracted using active contour without edges. (a) and (b) Perfectly segmented (whole tooth) (P); (c) and (d) Perfectly segmented crown (PC); (e) and (f) Erroneous contour can be corrected in the post-processing step (C); (g) and (h) Error in contour extraction (E).

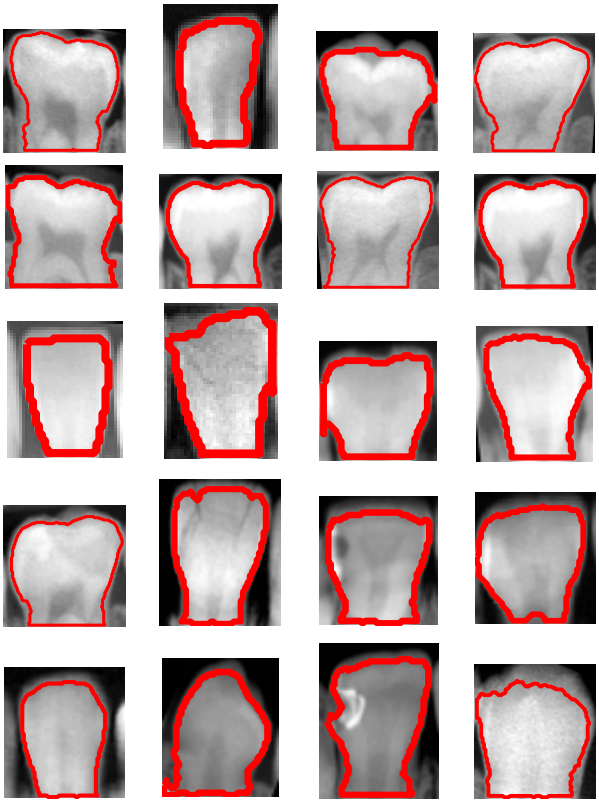

Fig. 5. Contour extraction of molars, pre-molars, canines and incisors using active contour without edges.

Table 1 summarizes the performance of the proposed contour extraction technique. Figure 5 shows the results that were obtained using this algorithm on molars, pre-molars, canines and incisors. As can be seen, a very smooth and accurate (i.e., tight) teeth contour is obtained using this algorithm. Also, the contour extraction procedure is extremely fast approximately 0.16 second/tooth [3].

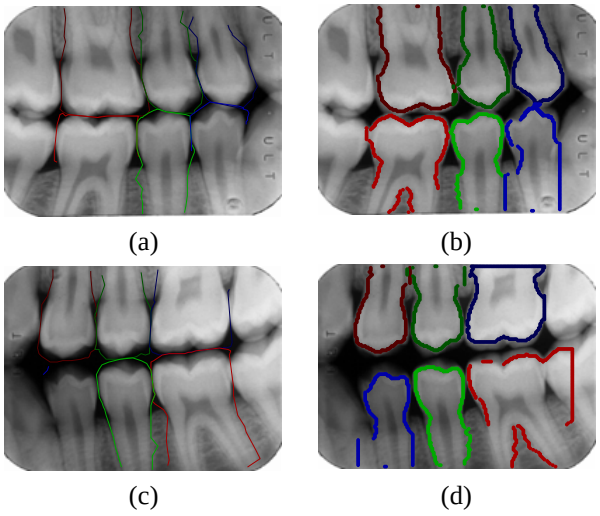

Fig. 6. Comparison of teeth contour extracted using snakes algorithm [5] and the proposed approach. (a) and (c) Contour extracted using the snake-based algorithm; (b) and (d) Contour extracted using active contour without edges. The primary difference between the two is the ability of the latter to elicit a tighter boundary than the former. Note that both algorithms are prone to errors. Extracting teeth contour from dental films is indeed a challenging task.

The snakes algorithm as implemented by Chen and Jain [6] was also used to extract the contour of the teeth images in dental films. Figure 6 (a) and (c) shows the contour extracted from two dental films using their technique. As is evident from the results, the snake is not able to detect the contour of many tooth entities in the dental films (e.g. lower left tooth in Figure 6 (c)). Also, the extracted contour does not fit tightly around the actual boundary of the teeth. This is perhaps due to the implicit limitations of the snake-based evolution techniques. The contour extracted for the same set of films using the proposed active contour without edges technique is shown in Figure 6 (b) and (d). It can be seen that the contours are extracted for most of the teeth in the films and they fit the boundaries rather tightly. The error in the extracted contour in Figure 6 (d) for the lower molar (red color) is due to incorrect teeth image segmentation in the previous stage. Figure 7 shows several examples of the extracted teeth contour on other films.

[3]The CPU-time was calculated in a MATLAB environment

1-4244-0487-8/06/$20.00 ©2006 IEEE

Records	Correct or partially correct contour extraction(%)			Errors in contour extraction (E)	Average time/tooth in seconds
	Perfect contour extraction (P)	Perfect crown contour extraction (PC)	Contour can be corrected at later stage (C)		
10 (AM)	56.2	14.05	16.75	13.0	0.15
10 (PM)	60.0	11.61	14.83	13.56	0.17
20 (Total)	58.10	12.83	15.79	13.28	0.16

Table 1. Performance of the proposed teeth contour extraction algorithm.

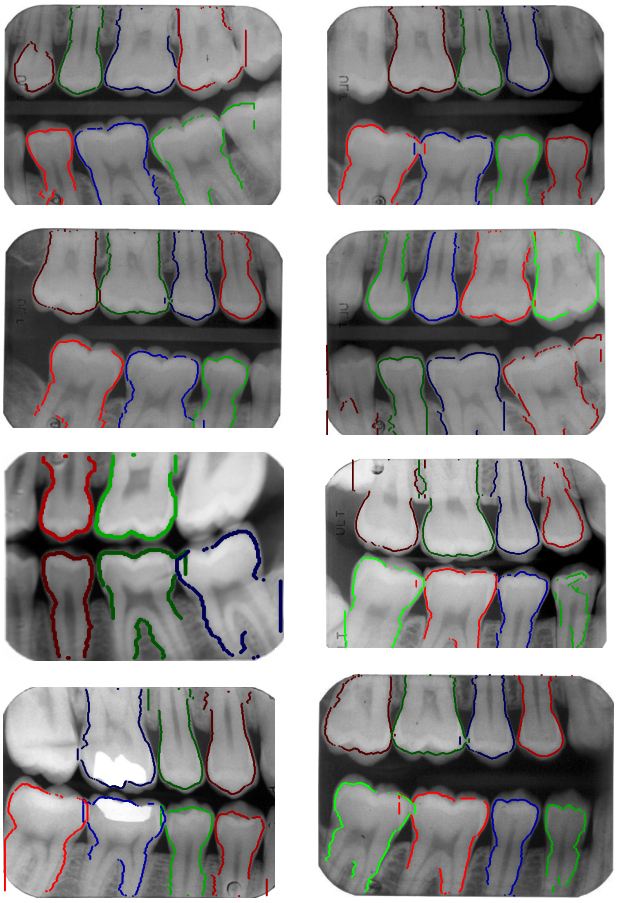

Fig. 7. A few more examples of segmentation using active contour without edges. As can be seen, some contours are in error.

4. SUMMARY AND FUTURE WORK

In this paper, an active contour without edges algorithm is used to extract the contour of teeth from dental images. This is an important component of any Automated Dental Identification System (ADIS). As digital X-ray images of the teeth usually do not exhibit sharp edges, the proposed algorithm is used to extract the tooth contour using a technique that depends on the intensity of the whole tooth region and not just the edges. Experimental results suggest the efficacy of the contour extraction process using the proposed technique. The plan for future work includes combining the results of multiple contour extraction algorithms to localize the teeth more accurately and to incorporate the segmentation routine in ADIS so as to facilitate tooth classification and matching in large-scale dental identification.

5. ACKNOWLEDGEMENTS

This work is supported in part by the U.S. National Science Foundation under Award number EIA-0131079 to West Virginia University; the research is also supported under Award number 2001-RC-CX-K013 from the Office of Justice Programs, National Institute of Justice, and the U.S. Department of Justice. Points of view in this document are those of the authors and do not necessarily represent the position of the U.S. Department of Justice. The authors wish to thank the Criminal Justice Information Services Division (CJIS) of the FBI for their support. The authors wish to thank Dr. Tim McGraw of West Virginia University for his valuable input.

6. REFERENCES

[1] A. Pretty and D. Sweet, "A look at forensic dentistry - part 1: The role of teeth in the determination of human identity.," *British Dental Journal*, vol. 190, no. 7, pp. 359–366, April 2001.

[2] G. Fahmy, D. M. Nassar, E. Haj Said, H. Chen, O. Nomir, J. Zhou, R. Howell, H. H. Ammar, M. Abdel-Mottaleb, and A. K. Jain, "Toward an automated dental identification system," *Journal of Electronic Imaging*, vol. 14, no. 4, pp. 1–13, 2005.

[3] X. Li, A. Abaza, D. M. Nassar, and H. H. Ammar, "Fast and accurate segmentation of dental x-ray records.," in *International Conference on Biometric (ICB)*, HongKong, January 2006, pp. 688–696.

[4] E. Haj Said, D. M. Nassar, and H. H. Ammar, "Image segmentation for automated dental identification," in *SPIE Electronic Imaging*, San Jose, CA, January 2006.

[5] A. K. Jain and H. Chen, "Matching of dental x-ray images for human identification," *Pattern Recognition*, vol. 37, no. 7, pp. 1519–1532, 2004.

[6] H. Chen and A. K. Jain, "Tooth contour extraction for matching dental radiographs," in *International Conference on Pattern Recognition (ICPR)*, Cambridge, UK, August 2004, pp. 522–525.

[7] M. Kass, A. Witkin, and D. Terzopoulos, "Snakes: Active contour models," *International Journal of Computer Vision*, vol. 1, no. 4, pp. 321–331, 1987.

[8] J. Zhou and M. Abdel-Mottaleb, "A content-based system for human identification based on bitewing dental x-ray images," *Pattern Recognition*, vol. 38, no. 11, pp. 2132–2142, 2005.

[9] R. Malladi, J. A. Sethian, and B. C. Vemuri, "Shape modeling with front propagation: A level set approach," *IEEE Transactions on Pattern Analysis and Machine Intelligence*, vol. 17, no. 2, pp. 125–133, February 1995.

[10] J. A. Sethian, "A review of recent numerical algorithms for hypersurfaces moving with curvature dependent speed," *Journal of Differential Geometry*, vol. 31, pp. 131–161, 1989.

[11] S. Osher and J. A. Sethian, "Fronts propagating with curvature-dependent speed: algorithms based on hamilton-jacobi formulations," *Journal of Computational Physics*, vol. 79, no. 1, pp. 12–49, 1988.

[12] Y.G. Chen, Y. Giga, and S. Goto, "Uniqueness and existence of viscosity solutions of generalized mean curvature flow equations," *Journal of Differential Geometry*, vol. 33, pp. 749–786, 1991.

[13] V. Caselles, R. Kimmel, and G. Sapiro, "Geodesic active contours," *International Journal of Computer Vision*, vol. 22, no. 1, pp. 61–79, 1997.

[14] T. F. Chan and L. A. Vese, "Active contours without edges," *IEEE Transactions on Image Processing*, vol. 10, no. 2, pp. 266–277, 2001.

[15] D. Mumford and J. Shah, "Optimal approximation by piecewise smooth functions and associated variational problems," *Communications on Pure and Applied Mathematics*, vol. 42, pp. 577–685, 1989.

[16] "CJIS division - ADIS, digitized radiographic images (database)," August 2002.

1-4244-0487-8/06/$20.00 ©2006 IEEE